ARTICLE OPEN

Check for updates

Genetics and Genomics

Attenuation of the CpG island methylator phenotype and lack of WNT signalling activation restrains *Kras* mutant intestinal neoplasia

Lochlan Fennell[1,2,3,4]✉, Cheng Liu[5,6], Alexandra Kane[5,7,8], Simon Tria[5], Jennifer Borowsky[5,7], Lu Chai[4], Sarron Randall-Demllo[4], Diane McKeone[5], Catherine Bond[5,7], Barbara Leggett[5,7,9] and Vicki Whitehall[5,7,8]

BACKGROUND: Serrated neoplasia arises from serrated precursor lesions. Hyperplastic polyps commonly activate MAPK signalling, initiated by *BRAF* or *KRAS* mutation, but premalignant *KRAS*-mutant sessile serrated lesions are rare. Here, we model *Kras*- and *Braf*-mutant neoplasia in vivo comparing histological, transcriptomic, and epigenetic changes.
METHODS: Temporospatial activation of oncogenic $Braf^{V637}$ or $Kras^{G12D}$ was induced in murine intestine. Differential expression, methylation and pathways analyses identified oncogene-specific alterations.
RESULTS: Prolonged exposure to oncogenic *Braf* is associated with a time-dependent accumulation of murine serrated precursors (mSP, $P = 3 \times 10^{-10}$), and murine serrated lesions (mSL) and invasive cancer (8×10^{-8}). *Kras*-mutants acquired fewer mSPs ($P = 0.06$) and lower probability of developing mSLs ($P = 0.004$). *Kras*-mutant mSLs rarely develop aberrant WNT signalling (1/23). Transcriptomic profiles diverged, with *Braf*-mutant intestines showing enriched immune and inflammatory signalling. Deconvolution analysis revealed *Braf*-mutants had comparably higher macrophage infiltrate ($P = 0.025$) and upregulation of M1 macrophage gene sets ($P = 0.0008$). Both mutations showed accumulating DNA methylation, however, an attenuated rate in a subset of CpG sites (1306) was observed in *Kras*-mutant intestine.
CONCLUSION: *Kras* mutation can induce serrated neoplasia, but with significantly greater latency period and lower penetrance compared to *Braf*. *Kras*-mutant neoplasms display an attenuated CIMP-like phenotype, rarely developing aberrant WNT signalling. These data refine our understanding of MAPK-induced intestinal neoplasia.

British Journal of Cancer (2026) 134:1230–1239; https://doi.org/10.1038/s41416-025-03271-3

INTRODUCTION

Serrated colorectal neoplasia is now accepted to be the molecular pathway underpinning ~25% of colorectal cancers. These cancers are associated with female gender, proximal colonic location and older age. Serrated colorectal cancers are also molecularly distinct from conventional pathway cancers. They are driven by *BRAF* mutation, rarely display chromosomal instability, and ~70% have a hyper-mutator phenotype. Serrated pathway colorectal cancers arise from sessile serrated lesions (SSLs) and less commonly traditional serrated adenomas (TSAs). SSLs are strongly associated with *BRAF* mutation, and rarely possess *KRAS* mutation. TSAs, by contrast, can be initiated by *BRAF* or *KRAS* mutation [1, 2] but are very uncommon. Both *BRAF* and *KRAS* reside in the MAPKinase signalling pathway, and their mutation results in increased proliferation, diminished apoptosis, and increased cell growth [3]. It is not clear why *KRAS* mutation does not appear to be sufficient to initiate serrated neoplasia via SSLs.

The CpG Island Methylator Phenotype (CIMP) is an important component of *BRAF* mutant serrated neoplasia. Several studies have implicated *BRAF* mutation directly in causing this phenotype. It is possible that *KRAS* mutation does not induce the degree of DNA hypermethylation required for progression of SSLs. This is supported by DNA methylation analysis of hyperplastic polyps. *BRAF* mutant hyperplastic polyps tend to have a microvesicular histological appearance [4], and can harbour molecular features that are similar to SSLs, such CIMP [5]. In contrast, most *KRAS* mutant hyperplastic polyps have a goblet-cell rich histological appearance, and rarely display CIMP [5]. These findings might

[1]School of Health, University of Sunshine Coast, Birtinya, QLD, Australia. [2]Centre for Bioinnovation, University of Sunshine Coast, Sippy Downs, QLD, Australia. [3]School of Pharmacy and Medical Sciences, Griffith University, Southport, QLD, Australia. [4]Oncogenic Aging Laboratory, Biomedicine Discovery Institute, Monash University, Clayton, VIC, Australia. [5]Conjoint Gastroenterology Laboratory; Cancer Faculty, QIMR Berghofer Medical Research Institute, Herston, QLD, Australia. [6]Envoi Specialist Pathologists, Kelvin Grove, QLD, Australia. [7]Faculty of Medicine, The University of Queensland, St Lucia, QLD, Australia. [8]Conjoint Internal Medicine Laboratory; Queensland Health, Pathology Queensland, Brisbane, QLD, Australia. [9]Department of Gastroenterology and Hepatology, Royal Brisbane and Women's Hospital, Herston, QLD, Australia. ✉email: lfennell@usc.edu.au

Received: 9 June 2025 Revised: 13 October 2025 Accepted: 14 November 2025
Published online: 23 February 2026

indicate that the lack of CIMP is a rate limiting step in serrated neoplasia via SSLs. Another critical step in the transition from SSL to cancer is the acquisition of molecular changes which increase WNT signalling [6].

Since both *KRAS* and *BRAF* act within the MAPKinase pathway such that mutations are mutually exclusive, it is not clear why serrated polyps initiated by *KRAS* mutation do not appear to have the same malignant potential as their *BRAF* mutant counterparts. Using a $Kras^{LSL\text{-}G12D}$ mouse model, Feng et al. [7] reported intestinal hyperplasia and an alteration in the cellular composition of intestinal crypts, but did not observe pre-malignant lesion formation. They attributed this to a lack in the expansion of the presumptive stem pool. This, and previous studies using *Kras* mutant mice, were medium term studies. It is possible that lesion formation is protracted in these models, and this has reduced the likelihood of detecting them.

In this study, we have performed a comprehensive, long-term comparative analysis of the histological, gene expression and DNA methylation alterations induced by oncogenic *Braf* and *Kras* in vivo to shed light on the differential role of MAPK mutations in the colorectum. We report substantial transcriptomic, epigenetic and histological differences underpinning *Braf* and *Kras* induced neoplasia, highlighting the divergent nature of the molecular evolution of neoplasia in these contexts.

METHODS

Murine models of serrated neoplasia

To contrast the effects of *Braf* and *Kras* mutation on the murine intestine we employed two transgenic murine models. The $Braf^{V637}$ (Jax strain #: 017837) and $Kras^{G12D\text{-}LSL}$ (Jax accession #008179) models are cre-inducible and facilitate the expression of the oncogenic $Braf^{V637E}$ and $Kras^{G12D}$ alleles, respectively. These are the murine analogues of the frequently mutated human $BRAF^{V600E}$ and $KRAS^{G12D}$ alleles, and recapitulate the constitutive oncogenic signalling that follows these mutations. These animals were crossed with Villin-Cre^{ERT2} (Jax strain #: 020282) mice, providing efficient spatiotemporal control over the recombination of the oncogenic alleles via a single intraperitoneal injection of tamoxifen (75 mg/kg). See Supplementary Table 1 for the number of experimental units for each group. Sample sizes were determined based on prior studies of *Braf* mutant mice. Animals were excluded if they did not survive to previously determined endpoints.

Immunohistochemistry

Immunohistochemistry was performed to assess the protein expression of β-Catenin and Ki67. For Ki67, 4 µm tissue sections were affixed to charged slides, dewaxed, and rehydrated. Peroxidase activity was blocked by incubating sections in 2% hydrogen peroxide in tris-buffered saline for 10 min. Antigens were retrieved by incubating sections in pH 6.0 Epitope Retrieval Solution (Dako, USA) at 125 °C for 3 min in a decloaking chamber. Sections were incubated in Background Sniper + 1% BSA (Biocare Medical, USA) to prevent spurious staining. Antibody was applied to sections for 60 min (1:100 dilution in Da Vinci Green (Biocare Medical); Ab Cat #ab16667). Stains were developed by incubating sections in MACH1 Rabbit HRP for 30 min and betazoid DAB for 5 min, and counterstained with Haematoxylin. Slides were scanned using an Aperio AT2 slide scanning instrument and analysed using QuPath using default cell segmentation and positive detection settings. β-Catenin immunohistochemistry was performed as per Kane et al. [8]. Briefly, 4 µM sections were mounted on charged slides, dewaxed with xylol and rehydrated via the descending graded alcohol method. Peroxidase activity was blocked as outlined above. To retrieve antigens, slides were incubated in Dako antigen retrieval solution (pH 6.0) for 5 min at 125 °C in a decloaking chamber. Non-specific binding was blocked using Background Sniper + 2.0% BSA (Biocare Medical, USA). Sections were then incubated with an anti-human β-Catenin monoclonal antibody diluted 1:500 in 2% BSA in TBS (Ab cat 32572) overnight at room temperature. Stains were developed by incubating sections in MACH2 Rabbit HRP for 30 min and betazoid DAB for 5 min, and counterstained with Haematoxylin. Sections were graded by an expert gastrointestinal pathologist (JB) as per Kane et al. [8], which included an assessment of staining intensity, extent and localization across lesions.

Nucleic acid extractions and next generation sequencing library preparations

At necropsy, fresh tissue samples were harvested from the small intestine and snap frozen in liquid nitrogen. DNA and RNA were extracted from ~30 mg of fresh-frozen tissue using the AllPrep DNA/RNA/Protein mini kit as per the manufacturer's instructions. Sample integrity and quantity was assessed using the TapeStation platform (Agilent Technologies, USA). DNA methylation was assessed via reduced representation bisulphite sequencing (RRBS). Libraries were generated using the Ovation RRBS Methyl-Seq library preparation kit (Tecan Genomics, USA) as previously reported (Fennell et al. [9]). Transcript expression was assessed via RNA-Seq using the Illumina Stranded Total RNA with RiboZero Plus kit (Illumina, USA) as per the manufacturers protocol.

RNA-sequencing data analysis

RNA-sequencing data was processed using nfcore RNAseq [10] nextflow pipeline (v3.0). This pipeline performs adaptor and quality trimming with Trim Galore! (v0.6.6), aligns reads to GRCm38 using STAR [11] (v2.6.1d), and quantifies genes and transcripts using Salmon [12] (v1.4.0). The pipeline generates various quality control metrics using tools including RSeQC [13] (v3.0.1), Qualimap [14] (v2.2.2), FastQC (v0.11.9), dupRadar [15] (v1.18.0), and Preseq (v2.0.3). Differential gene expression analysis was performed using DeSeq2 [16] (v3.13). To estimate and compare cell type proportions we deconvoluted the bulk RNAseq data using ImmuneCC, a reference-based deconvolution method, and the standard immune signature matrix. To prepare the data for this analysis we performed TMM normalisation on raw counts using EdgeR (v3.4.2). Data was kept in linear space as per best practice for bulk deconvolution.

Reduced representation bisulphite sequencing data analysis

RRBS reads were trimmed to remove adaptors and poor quality sequences using Trim Galore! (v0.6.6). NuGen diversity adaptors were removed using the custom 'trimRRBSdiversityAdaptCusomters.py' script [17]. Reads were then aligned and methylation calls generated using the methylseq nf-core pipeline (v2.3.0). This pipeline employs Bismark for methylation aware sequence alignment and extraction, and qualimap and preseq for generating quality control metrics. Principal components analysis was performed using the 'prcomp' R function. Differential DNA methylation analysis was performed using Limma (v3.56.2) and differential methylation results were considered significant if the absolute methylation difference in contrasts was >20% and the FDR < 0.05. The methylGSA (v1.18.0) method was employed for gene ontology enrichment analysis using the robust rank aggregation method with CpGs mapping to promoters (distance to transcription start site: −1500 to +100 bp) as input. This method adjusts for the extreme biases that exist when performing gene set analysis on DNA methylation data by virtue of the unequal distribution of CpGs in the promoters of protein coding genes. To assess age associated DNA methylation we performed linear regression analysis using the 'lm' R function. We then assessed for mutation specific differences in age-associated DNA methylation by analysis of covariance.

Statistical analyses

All statistical analyses were performed using R (v4.0.3). Results were reported as significant if $p < 0.05$. *P* values were corrected using the false discovery rate method, where appropriate.

RESULTS

Oncogenic Braf and Kras mutation induces differentially penetrant murine serrated neoplasia

BRAF and *KRAS* mutation are common mutational events in human serrated colorectal neoplasia. To test whether mutation of *BRAF* or *KRAS* is sufficient to initiate serrated neoplasia we employed the spatiotemporally inducible $Braf^{V637}$ and $Kras^{G12D}$ murine models (see methods for more detail).

In $Braf^{V637}$ mice, we observe a steady and significant temporal accumulation of murine serrated precursors ($R^2 = 0.56$, $P = 3 \times 10^{-10}$; Fig. 1a). These lesions display crypt dilatation and mucinous differentiation, consistent with previous studies [18]. *Kras* mutant mice, by contrast, accumulated lesions at a much slower rate ($R^2 = 0.22$, $P = 0.04$; Fig. 1a) and were rare even in

those exposed to *Kras* mutation for 14–18 months. For *Kras* mutant animals, precursors were significantly more common in male animals at all time points except 10 days (Supplementary Table S2).

Both models developed advanced serrated lesions, which display overt cytological dysplasia; however the frequency and rate at which these lesions developed differed substantially between the models. Lesions were confined to the duodenal and jejunal regions of the small intestine. we did not observe differences in the regional distribution of lesions between models. The probability of *Braf* mutant animals developing an advanced serrated lesion increased substantially from ~25% in five-month animals to >95% in 14 month animals. In contrast, the probability of *Kras* mutant animals developing advanced serrated neoplasia increased significantly more slowly with age (Logistic regression interaction model $P = 0.004$; Fig. 1b). At the 14 month time point, the probability of a *Kras* mutant animal developing advanced serrated neoplasia was 66% lower than age matched *Braf* mutant animals (28% vs 94%; Fig. 1b). We did not observe conventional adenomas in either model. Therefore, both *Braf* and *Kras* mutation can induce serrated neoplasia, however the *Braf* mutation has a significantly higher penetrance.

BRAF mutant human cancers tend to occur more frequently in female individuals, and *KRAS* mutant cancers have a preponderance for males. Thus, we next sought to assess whether there were any gender biases present in our murine models. *Braf*-induced advanced serrated neoplasia at the same frequency in male and female animals (Fig. 1d). However, *Kras*-induced serrated neoplasia occurred almost exclusively in male animals ($P < 0.0001$), with only one *Kras* mutant female animal developing an advanced serrated lesion in the entire study. When segregated by gender, *Kras* mutant male animals had a 79% chance of developing advanced serrated neoplasia at 18 months (Fig. 1).

Kras mutation induces less severe hyperplasia, but greater crypt proliferation when compared with *Braf* mutation

To examine whether proliferative activity might underpin the histological differences we observe in the manifestations of both mutations, we evaluated the extent of hyperplasia in the *Braf* and *Kras* mutant intestines. First, we examined the length of the small intestine of all animals in the study. These measurements were recorded at necropsy. At all timepoints assessed in both models (10 days to 14 months), the *Braf* mutated intestine was significantly longer as compared with *Kras* mutant animals (ANOVA $P = 0.0002$). Male *Kras* mutant animals had significantly longer small intestines than female *Kras* mutant animals (ANOVA $P = 6.83 \times 10^6$, mean difference 3.63 cm), however there was no specific interaction between sex and intestine length in *Braf* mutant animals (ANOVA $P = 0.18$). Next, we measured the length of the small intestinal villi of a subset of animals (15 villus per animal). In keeping, we observed that the length of the villi of *Kras* mutant animals was significantly shorter when compared with age-matched *Braf* mutant mice (Fig. 2a). We did not observe any sex specific differences in villus length in either setting. These data indicate that *Braf* mutation induces greater hyperplasia when compared with *Kras* mutation.

Next, we sought to examine whether the more severe hyperplasia observed in *Braf* mutant animals might be explained by greater proliferative activity in the intestinal crypts. Ki67 accumulates in the nucleus during the cell cycle and is a surrogate marker of proliferation. We performed immunohistochemical analysis of intestinal sections to compare the proliferation of *Braf* and *Kras* mutant mice. At all time points, we observed significantly greater proliferation in the crypts of *Kras* mutant compared with *Braf* mutant animals (Fig. 2b, c; Two-way ANOVA $P = 4.75 \times 10^6$, 0.0013, and 0.024 at 2, 8 and 14 months, respectively).

WNT signalling hyperactivation is not a feature of Kras mutant serrated lesions

WNT signalling activation is a hallmark of colorectal neoplasia. We have previously shown that *Braf* mutant lesions acquire dysregulated WNT signalling via mutation of *CTNNB1*, which results in a concomitant translocation of β-catenin to the nucleus and activation of WNT-target genes [8, 18]. To test whether WNT signalling is similarly deregulated in *Kras* mutant serrated neoplasia, we performed immunohistochemical analysis on murine serrated lesions ($n = 16$ animals, $n = 23$ total lesions). Abnormal β-catenin staining was observed in 1/23 lesions assessed (Fig. 3a). This lesion displayed weak focal nuclear β-catenin affecting <10% of nuclei in the lesion (Fig. 3b). This lesion arose in a 14 month old animal. The remaining lesions displayed a normal membranous staining pattern. By contrast, we previously reported that 40% and 100% of *Braf* mutant mSLs had abnormal β-catenin staining 10 and 14 months, respectively [8]. These animals are a subset of those presented in this manuscript. For comparison, an immunohistochemical image of a murine serrated lesion arising in a 14 month *Braf* mutant animal is presented in Fig. 3c. These data indicate that abnormal WNT signalling activation is not a feature of murine serrated lesions that arise in the setting of *Kras* mutation.

Temporal divergence of the intestinal transcriptome in *Braf* and *Kras* mutant samples

Next, we sought to examine whether different signalling pathways are activated upon mutation of *Braf* when compared with mutation of *Kras*. We performed RNAseq on animals *Kras* and *Braf* mutant intestinal samples at 2, 8 and 14 months post mutation activation ($n = 3$ animals/genotype/timepoint).

Differential gene expression analysis revealed 148 differentially expressed genes between 2 month old *Kras* and *Braf* mutant samples (Absolute LogFC >2, FDR < 0.05), of which 38 were overexpressed in *Kras* mutant samples, relative to *Braf* mutant samples, and 110 underexpressed (Table 1 and Fig. 4a). At the 8 month timepoint, we observe significantly altered gene expression in 1023 genes. In keeping, the majority (790 genes, Table 1) were underexpressed in *Kras* mutant samples, with 233 genes being expressed to a greater degree in *Kras* mutant samples (Table 1 and Fig. 4a). By 14 months, 557 genes were differentially regulated, with 328 genes being underexpressed and 229 overexpressed in *Kras* mutant samples relative to age-matched *Braf* mutant samples (Table 1 and Fig. 4)). These data indicate that some loci are immediately differentially regulated in response to either *Kras* or *Braf* mutation, while others require sustained oncogenic exposure to manifest.

To explore the functional consequences of the disparate gene expression profiles of the *Kras* and *Braf* mutated intestine, we performed gene ontology enrichment analysis on genes differentially regulated at ≥2 time points. For genes that were downregulated in the *Kras* mutant intestine relative to *Braf* mutant animals, 203 were downregulated at ≥2 time points (Fig. 4b—Venn Diagrams). This geneset was enriched for several immune related processes, including the immune response (Observed/Expected ratio: 2.84, FDR corrected $P = 0.002$), innate immune response (Observed/Expected ratio: 2.37, FDR corrected $P = 0.003$), and positive regulation of the immune response (Observed/Expected ratio: 3.84, FDR corrected $P = 0.015$). Other enriched processes include the metabolic process (Observed/Expected ratio: 1.51, FDR corrected $P = 0.041$), and positive regulation of NF-kappa beta transcription factor activity (Observed/Expected ratio: 7.77, FDR corrected $P = 0.047$). For genes upregulated in *Kras* mutant samples, 62 were upregulated at ≥2 time points, however enrichment analysis did not identify any biological processes associated with these genes.

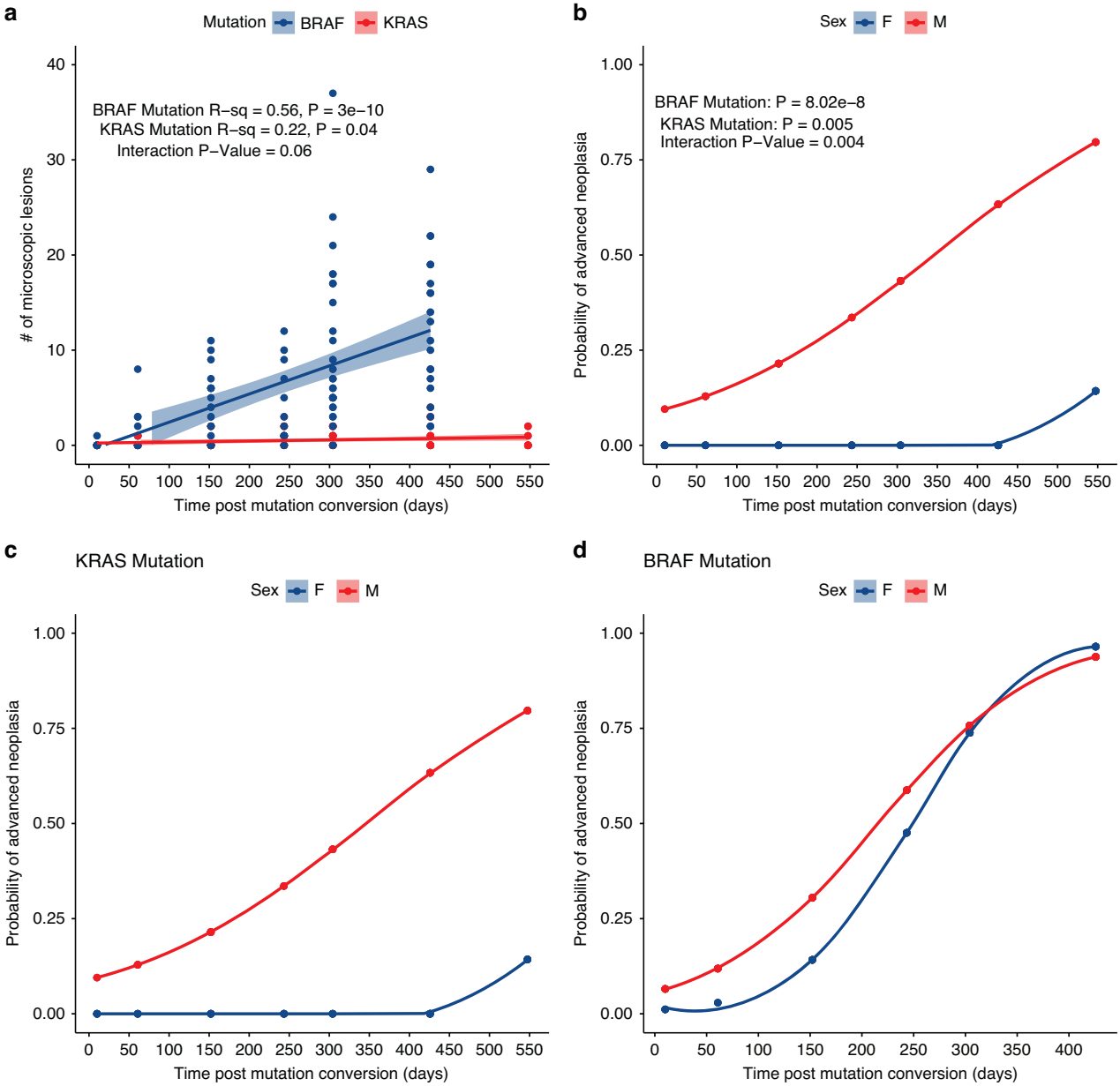

Fig. 1 Histopathological comparison of the Braf and Kras mutant intestine. a Number of microscopic lesions detected in Braf and Kras mutant animals aged from 10 days to 18 months. **b** The probability of advanced serrated neoplasia developing as a function of age and time exposed to each oncogene from wean. **c**, **d** Sex specific probability of advanced serrated neoplasia as a function age and time exposed to each oncogene from wean. Note that advanced neoplasia specifically refers to serrated neoplasia, as conventional adenomas were not observed in either model.

Immune cell deconvolution analysis reveals a *Braf*-mutation induced macrophage-inflamed response in the small intestine

Our earlier analysis revealed a strong immunological response in the *Braf* mutant intestine. We examined the immune contexture of the intestine of *Braf* and *Kras* mutant intestine by deconvoluting bulk RNAseq data using ImmuneCC (Fig. 5a). This analysis leverages known gene signatures to provide an estimate of the proportional abundances of specific immune cells given a bulk RNAseq dataset. Deconvolution analyses indicated a significant reduction in macrophage infiltrate in the microenvironment of the *Kras* mutant intestine when compared with *Braf* mutant mice ($P = 0.02$, Fig. 5b). The proportion of other immune cell types was not significantly different. We do note that some animals show a striking CD4+ T cell signature (Fig. 5a), however this was not altered between *Braf* and *Kras* mutant animals.

Macrophages can be polarised into a M1 (pro-inflammatory) and M2 (anti-inflammatory state). To characterise whether *Braf* mutation could induce an M1 macrophage polarisation phenotype we performed geneset enrichment analysis using previously published signatures from M1 and M2 macrophages. We observed significant enrichment for M1 inflammatory macrophage gene signatures in the *Braf* mutant model relative to *Kras* mutant mice ($P = 0.1$ and $P = 0.008$ for upregulated and downregulated genes that differentiate between M1 and M2 macrophages, respectively), in keeping with our observation that inflammatory processes and macrophages are enriched in the *Braf* mutant model (Fig. 5c). We also observed a significant difference in enrichment scores for genesets associated with regulation of macrophage apoptosis ($P = 0.0012$ and Fig. 5c) and macrophage activation ($P = 0.011$ and Fig. 5c). These data indicate that M1 macrophages may be

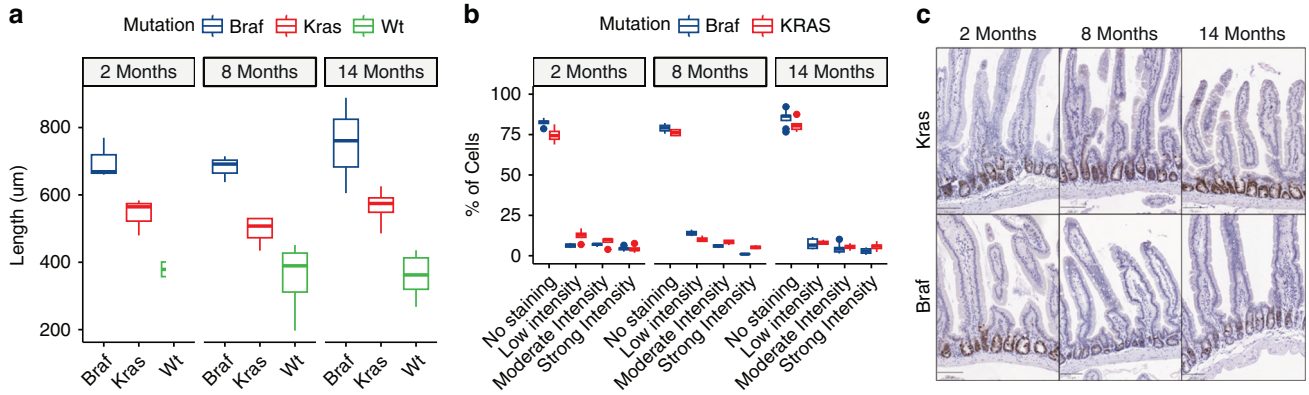

Fig. 2 Immunohistochemical comparison of Braf and Kras mutant intestine. a Mean Villus length of Braf, Kras and WT animals at two, eight and fourteen months. For each animal 15 villi were measured by a blinded operator. **b** Proliferative activity in the Braf and Kras intestines as measured by Ki67 immunostaining. (Braf: $n = 7$, 3 and 12 for 2 months, eight months and fourteen months, respectively; Kras: $n = 4$, 4, and 6 for 2, 8 and 14 months, respectively). **c** Representative images of Ki67 staining in Braf and Kras mutant animals at 2, 8 and 14 months.

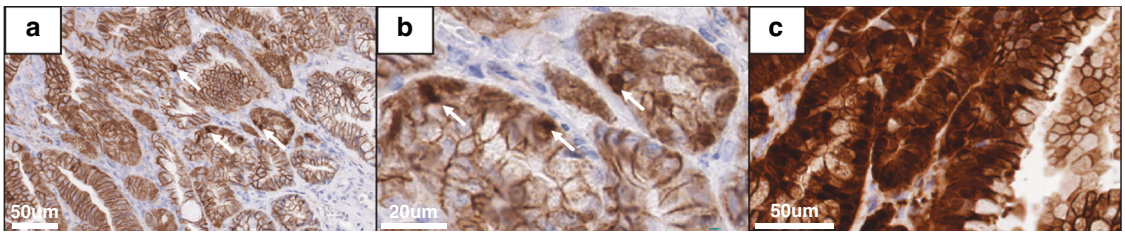

Fig. 3 β-catenin localisation differs in Kras mutant mSLs. a, **b** β-catenin immunohistochemistry showing focal nuclear localization of β-catenin (arrows) in the sole Kras mutant murine serrated lesion where abnormal β-catenin was identified. Typical membranous staining is observed throughout the remainder of the lesion. **c** β-catenin immunohistochemistry showing intense β-catenin expression and nuclear localisation in a 14 month old Braf mutant murine serrated lesion. Brown staining: DAB Blue staining: Hematoxylin.

Table 1. Differentially expressed genes in comparisons of the Kras and Braf mutant intestine at 2, 8 and 14 months.

Timepoint	Number of genes		
	Overexpressed[a]	Underexpressed[a]	Sum
2 months	38	110	148
8 months	233	790	1023
14 months	229	328	557

Differential gene expression analysis was performed using the DEseq2 R package. Genes with an absolute logFC >2 and an FDR < 0.05 were deemed significant.
[a]Over (Under) expressed in *Kras* mutant samples relative to *Braf* mutant samples.

enriched in the hyperplastic intestinal mucosa of *Braf* mutant mice and may contribute to chronic inflammatory signals that drive lesion initiation.

Intestinal Kras mutation is typified by an attenuation of the CpG island methylator phenotype

In human colorectal cancers both *KRAS* and *BRAF* mutation are linked to the CIMP, however, we have previously reported differences in the methylation spectrum by mutation. We hypothesise that differences in the degree and extent of CIMP in these animals may explain the differential risk of transformation associated with each oncogene. To test this, we performed genome-scale DNA methylation analysis by RRBS ($n = 3$ animals/genotype/timepoint; $n = 3$ WT animals/timepoint).

First, we sought to explore the genome-wide implications of *Braf* and *Kras* mutation by performing principal components analysis (Fig. 6a). PC1, explaining ~10% of the variance in the data, was correlated with age in the wild-type animals. This represents 'epigenetic drift'. In keeping with our earlier work, *Braf* mutant animals appear to accelerate endogenous aging, as evidenced by their accelerated divergence from wild-type animals across PC1 (Fig. 6a). *Kras* mutant animals showed a similar acceleration of endogenous aging, however, this was attenuated when compared with age-matched *Braf* mutant animals (Fig. 6a).

To examine the interaction between each mutation and age, we performed ANCOVA analysis on CpGs associated with age. Of the 27,957 CpGs that were associated with age in *Braf* mutant animals (FDR < 0.05), 55.1% were also associated with temporal shifts in DNA methylation in the intestine of *Kras* mutant animals. The rate of change in DNA methylation over time was significantly different in 1306 of these sites (Fig. 6b), with most sites accumulating DNA methylation at a slower rate in *Kras* mutant animals, providing further evidence for an attenuation of the CIMP.

The discrepancy in the incidence of advanced serrated neoplasia between *Braf* and *Kras* mutant animals is most apparent at 14 months (Fig. 1b). To understand the DNA methylation dynamics at this timepoint we performed differential DNA methylation analysis. We identified 2231 differentially methylated CpG sites (FDR < 0.05, |Δ| methylation >20), of which 1803 and 428 were comparably hypermethylated and hypomethylated in *Braf* mutant mice, respectively. Gene ontology enrichment analysis of genes that are comparably less methylated in the *Kras* mutant mice compared with *Braf* mutants revealed 81 significantly enriched terms (Fig. 6c). This included terms associated with differentiation, response to growth factors, WNT signalling, proliferation and cell-junction formation. Collectively, these data indicate that while *Kras* mutation induces widespread DNA hypermethylation, the severity and extent of methylation is lower when compared to that induced by *Braf* mutation.

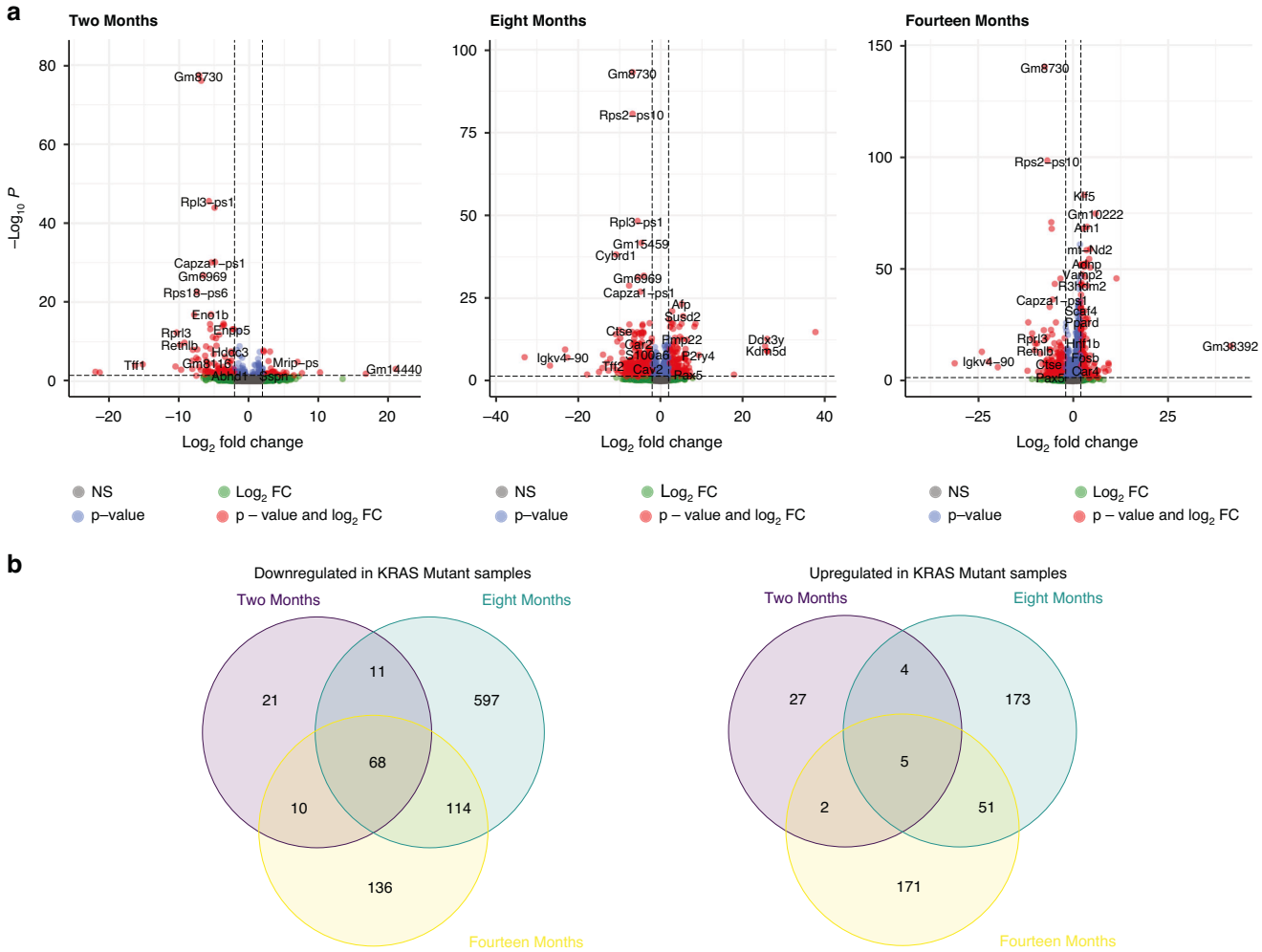

Fig. 4 Gene expression profiles show disparate signalling in the Braf and Kras mutant intestine. a Differential gene expression analysis comparing the expression profiles of Braf and Kras mutant at 2, 8 and 14 months. **b** Venn diagrams displaying the overlap between differentially expressed genes at 2, 8 and 14 months.

DISCUSSION

Both *BRAF* and *KRAS* are important oncogenic drivers in multiple cancer types including colorectal cancer. Mutation of these genes is common in colorectal cancer and both drive overactivation of the MAPK signalling pathway, resulting in heightened proliferative activity, dysregulated differentiation, and evasion of apoptosis. They are mutually exclusive presumably because they act within the same pathway. Here, we have comprehensively assessed the propensity for mutation in *Braf* and *Kras* to induce spontaneous neoplastic transformation in murine models. The penetrance of neoplasia was substantially lower in *Kras* mutant mice, and invasive cancer formation was rare. We observe a striking association between neoplasia and gender in *Kras*, but not *Braf* mutant mice, with neoplasia more likely to occur in male animals. Our transcriptomic and DNA methylation analysis revealed differences in immune expression profiles and regulation of genes associated with key signalling axis and biological processes. We show a novel attenuation of the CIMP and a distinct lack of WNT signalling dysregulation in *Kras* mutant mice. These findings shed light on differences in the natural course of polyps initiated by *Braf* and *Kras* mutation and highlight the restraints on the ability of mutant *Kras* to induce serrated pathway colorectal cancer.

Serrated neoplasia is hallmarked by overactivation of the MAPK signalling pathway [19], and widespread DNA methylation alterations [3, 20, 21]. Hyperplastic polyps are common, small serrated polyps which are not considered to have significant malignant potential and can be initiated by either BRAF or KRAS mutations. The serrated lesions which have risk of malignant potential are SSLs and TSAs. SSLs usually harbour *BRAF* V600E mutation, however the much rarer TSAs can activate MAPK via *KRAS* mutation in the context of additional genetic alterations which perturb BMP and WNT signalling [22–24]. Interestingly, the 75% of colorectal cancers which arise from conventional adenomas initiated by *APC* mutations which perturb WNT signalling, often have *KRAS* mutations but very rarely *BRAF* mutations. In the context of conventional adenomas, *KRAS* mutations occur in advanced adenomas which are likely to transition to invasive cancers. It has never been fully understood why there is selective advantage for either *BRAF* and *KRAS* mutations in particular polyp types when both oncogenes activate the same pathway.

To examine the mechanics of *BRAF* and *KRAS* induced neoplasia, we induced the murine analogues of these mutations in the intestine of mice at weaning and monitored the temporal development of histological manifestations thereafter. Animals with *Braf* mutation spontaneously developed neoplasia with complete penetrance by 14 months, consistent with our prior work [18, 25]. By contrast, less than 50% of *Kras* mutant animals developed advanced neoplasia. This finding is consistent with previous literature indicating a limited capacity for *Kras* to induce

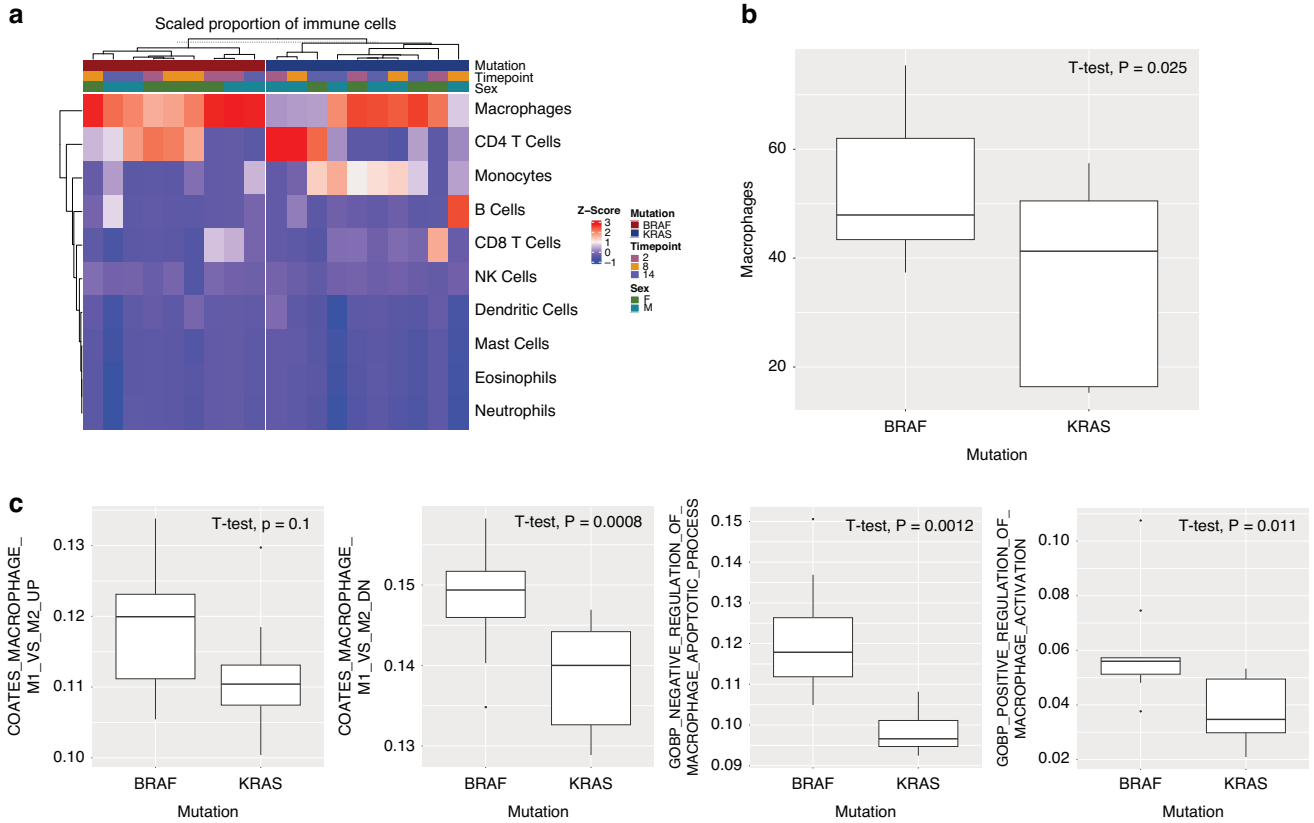

Fig. 5 RNA-based immune cell deconvolution reveals differences in immune cell abundance in the Braf and Kras mutant intestine. **a** Relative abundance of immune populations in Braf and Kras mutant animals as measured via deconvolution of bulk RNA sequencing data. Each heatmap cell represents the z-score normalised relative abundance of specific immune populations as determine via computational deconvolution analysis with ImmuneCC. **b** Relative abundance of macrophages as a fraction of all immune cells in the intestine of Braf and Kras mutant animals. **c** Gene set enrichment analysis for gene sets involved in macrophage activation, and apoptosis. Y axis corresponds to the enrichment score associated with each pathway.

intestinal neoplasia in mice [7]. Feng and colleagues reported that *Kras* mutation induces overt proliferation and crypt hyperplasia, but not premalignant lesion formation or dysplasia. Our histological analysis confirms the former but disputes the latter. In our study, a subset of animals developed overtly dysplastic serrated lesions, however the *Kras* mutant animals in our study were aged–18 months. These data indicate that the sojourn from mutation to lesion formation may proceed over a long period of time and that human *KRAS* initiated serrated neoplasia might follow a similarly protracted evolution.

We also examined the beta catenin/WNT signalling axis by immunohistochemistry. *Braf* mutant murine serrated neoplasia is predicated upon the spontaneous activation of WNT signalling via *Ctnnb1* mutation [8]. Early *Braf* mutant lesions rarely mutate *Ctnnb1*, however by 14 months all animals displayed some form of *Ctnnb1* mutation. In humans, we observe mutation of *APC* or *RNF43* in dysplastic SSLs and serrated pathway cancers, with the former being more common in mismatch repair proficient cancers. *APC* is a member of the WNT pathway in keeping with our model system [6, 26]. Here, we report significant accumulation of beta catenin in lesions from *Braf*, but not *Kras* mutant mice. Future studies might address whether the lack of beta catenin nuclear translocation in this setting limits the expression of WNT target genes that are important for neoplastic transformation.

The CIMP can occur in both *BRAF* and *KRAS* mutant colorectal cancers. CIMP has been linked to the silencing of key tumour suppressor genes, fuelling cancer initiation and progression. We previously reported distinct subtypes of CIMP-High colorectal cancers, marked by differential mutational frequency of *BRAF* and *KRAS* [20]. To evaluate the extent to which *Braf* and *Kras* mutation induce different DNA methylation patterns, we performed genome-scale methylation analysis on the intestine of mice. While both *Braf* and *Kras* mutant mice develop significant aberrant DNA methylation, the phenotype is less severe and somewhat attenuated in the *Kras* mutant intestine. This is consistent with the delayed development of neoplasia in these animals. *KRAS* mutation is common in human hyperplastic polyps and *BRAF* mutation is common in SSLs. *KRAS* mutant hyperplastic polyps are rarely CIMP-high [5]. By contrast, ~70–80% of *BRAF* mutant SSLs harbour the CIMP [27]. Collectively, these data indicate that the attenuation and delayed development of CIMP may restrain *KRAS* mutant polyps and prevent their progression to cancer unless the KRAS mutation occurs in the context of pre-existing significant other mutations perturbing pathways such as WNT.

Despite inducing neoplasia with significantly lower penetrance, we observed elevated Ki67 expression in the crypt compartment of *Kras* mutant mice, indicating greater proliferative activity. This finding appears counterintuitive, but may be explained by the competition dynamics that underpin lesion formation in the gut. We and others have reported that WNT signalling is perturbed during aging [25, 28, 29], resulting in decreased stemness and regenerative capacity [30, 31]. We have also previously reported that WNT pathway members become hypermethylated during aging and that this process is hastened by *Braf* mutation [25]. Flanagan and colleagues [32] recently reported on the role the competition dynamics in the intestine that allow for the formation of *Apc* mutant lesions. They show that NOTUM, a potent secreted WNT antagonist, inhibits WNT signalling in non-neoplastic crypts

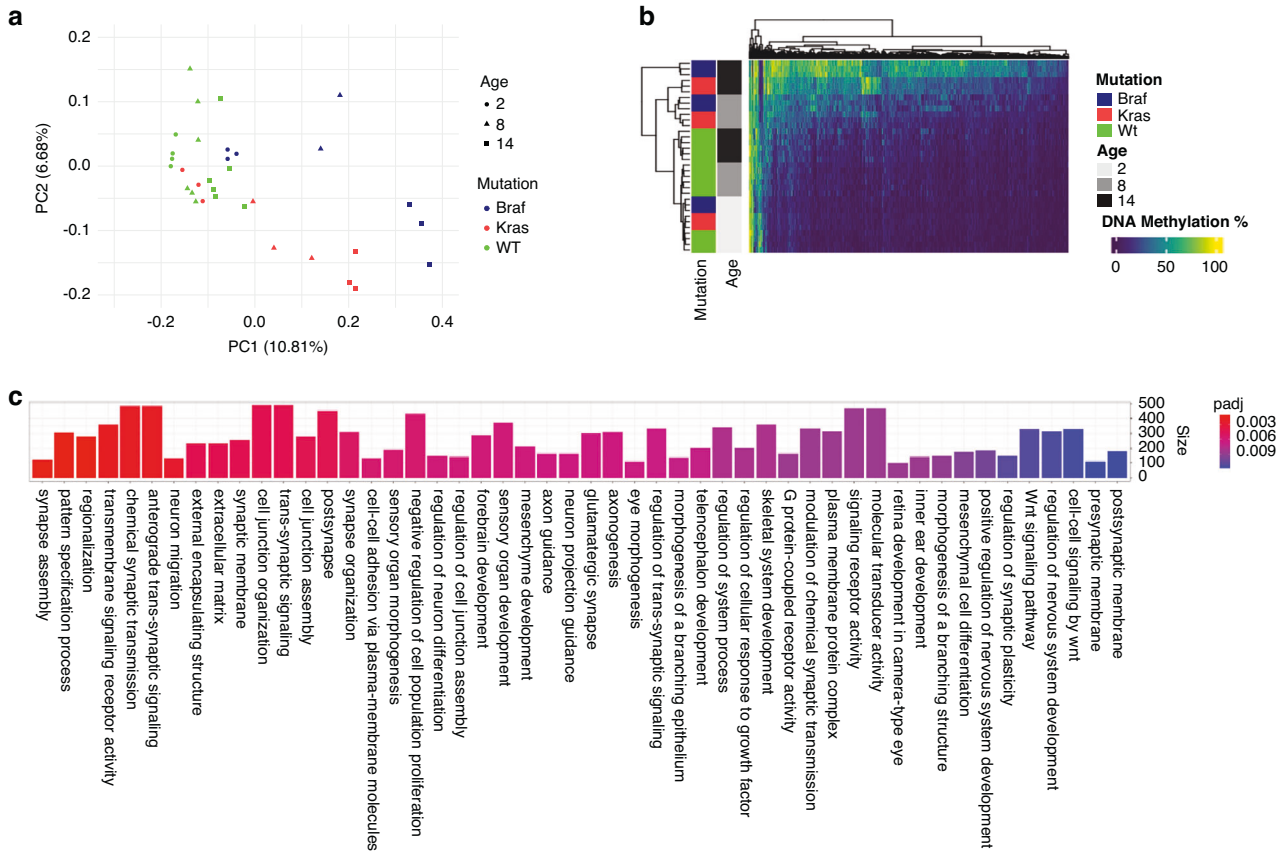

Fig. 6 The CpG island methylator phenotype and age associated DNA methylation is attentuated in the Kras mutant intestine. a Principal components analysis of the entire methylome of Braf, Kras and WT animals. PC1 is strongly associated with age and exposure time to either Braf or Kras. **b** Heatmap depicting 1306 CpG sites that show a significantly different temporal methylation trajectory between Braf and Kras mutant animals. **c** Gene ontology analysis of differentially hypermethylated genes in Braf mutant animals compared with Kras mutant animals at 14 months.

that neighbour lesions [32]. This reduces their competitiveness and allows lesions to fix and expand. It is possible that the sustained elevation of proliferation in the *Kras* mutant crypts inhibits the formation of lesions by outcompeting lesions when they are initiated. In the *Braf* mutant intestine, which has comparably lower proliferation and stronger transcriptomic and epigenetic repression of WNT signalling and stemness, new lesions may have a competitive advantage and be able to form more readily. The precise role of competition dynamics in the serrated pathway warrant further investigation.

Our transcriptomic analyses revealed several genomic differences between the *Kras* and *Braf* mutated intestine. We note that the *Braf* mutant intestinal transcriptome is characterised by upregulation of immunological pathways, consistent with an inflammatory phenotype. To understand this we performed deconvolution analysis, revealing a significantly higher contribution of macrophages to the overall transcriptomic profile of these animals. Tissue resident macrophages can adopt pro- or anti-inflammatory phenotypes [33]. Gene set enrichment analysis confirmed an upregulation of pro-inflammatory M1 macrophage gene expression programs, and concomitant decrease in apoptosis and increase in macrophage activation. Whether M1 macrophages promote or suppress neoplasia is context dependent. In established tumours, M1 macrophages are generally associated with tumour suppressive capabilities, owing to their secretion of pro-inflammatory cytokines which can enhanced tumour killing [34, 35]. By contrast, in inflammatory disorders they may promote tumour initiation by fostering a mutagenic microenvironment and promoting the generation of reactive oxygen species [36, 37]. It is possible that chronic inflammatory signalling, induced by increased abundance of M1 macrophages, may damage the epithelium and contribute to the increased propensity for neoplastic transformation in the intestine of *Braf* mutated animals.

Here we performed a comprehensive analysis of the impacts of both *Braf* and *Kras* mutation on the intestinal epithelium using transgenic murine models. *Braf* mutation induces serrated neoplasia, accompanied by temporal dysregulation of the transcriptome and epigenome, with high penetrance. We observed functional enrichment of immune related processes in the *Braf* mutant intestine, which may be mediated by pro-inflammatory macrophages in the microenvironment. *Kras* mutation does result in premalignant lesion formation, however with a significantly protracted latency period, and attenuated transcriptomic and epigenomic alterations, and a lack of aberrant WNT signalling activation. These data shed light on the differential role of *Braf* and *Kras* mutation in the gut and provide clarity around why *Braf* mutation induces serrated pathway cancers, while *Kras* mutant serrated cancers are rare.

Reporting summary

Further information on research design is available in the Nature Research Reporting Summary linked to this article.

DATA AVAILABILITY

The datasets generated and/or analysed during the current study are available from the corresponding author on reasonable request.

REFERENCES

1. Chan TL, Zhao W, Leung SY, Yuen STCancer Genome Project. BRAF and KRAS mutations in colorectal hyperplastic polyps and serrated adenomas. Cancer Res. 2003;63:4878–81.
2. Yang S, Farraye FA, Mack C, Posnik O, O'Brien MJ. BRAF and KRAS Mutations in hyperplastic polyps and serrated adenomas of the colorectum: relationship to histology and CpG island methylation status. Am J Surg Pathol. 2004;28:1452–9.
3. Bond CE, Whitehall VLJ. How the BRAF V600E mutation defines a distinct subgroup of colorectal cancer: molecular and clinical implications. Gastroenterol Res Pract. 2018;2018:e9250757.
4. Juárez M, Egoavil C, Rodríguez-Soler M, Hernández-Illán E, Guarinos C, García-Martínez A, et al. KRAS and BRAF somatic mutations in colonic polyps and the risk of metachronous neoplasia. PLoS ONE. 2017;12:e0184937.
5. Fernando WC, Miranda MS, Worthley DL, Togashi K, Watters DJ, Leggett BA, et al. The CIMP phenotype in BRAF mutant serrated polyps from a prospective colonoscopy patient cohort. Gastroenterol Res Pr. 2014;2014:e374926.
6. Borowsky J, Dumenil T, Bettington M, Pearson SA, Bond C, Fennell L, et al. The role of APC in WNT pathway activation in serrated neoplasia. Mod Pathol. 2018;31:495–504.
7. Feng Y, Bommer GT, Zhao J, Green M, Sands E, Zhai Y, et al. Mutant Kras promotes hyperplasia and alters differentiation in the colon epithelium but does not expand the presumptive stem cell pool. Gastroenterology. 2011;141:1003–e10.
8. Kane AM, Fennell LJ, Liu C, Borowsky J, McKeone DM, Bond CE, et al. Alterations in signalling pathways that accompany spontaneous transition to malignancy in a mouse model of BRAF mutant microsatellite stable colorectal cancer. Neoplasia. 2020;22:120–8.
9. Fennell LJ, Hartel G, McKeone DM, et al. Comparative analysis of Illumina Mouse Methylation BeadChip and reduced-representation bisulfite sequencing for routine DNA methylation analysis. Cell Rep Methods. 2022;2:100323.
10. Patel H, Ewels P, Peltzer A, Hammarén R, Botvinnik O, Sturm G, et al. nf-core/rnaseq: nf-core/rnaseq v3.0 - Silver Shark. Zenodo; 2020 [cited 2021 Jun 29]. Available from: https://zenodo.org/record/4323183
11. Dobin A, Davis CA, Schlesinger F, Drenkow J, Zaleski C, Jha S, et al. STAR: ultrafast universal RNA-seq aligner. Bioinformatics. 2013;29:15–21.
12. Patro R, Duggal G, Love MI, Irizarry RA, Kingsford C. Salmon: fast and bias-aware quantification of transcript expression using dual-phase inference. Nat Methods. 2017;14:417–9.
13. Wang L, Wang S, Li W RSeQC: quality control of RNA-seq experiments. Bioinform Oxf Engl. 2012 Aug 15 [cited 2021 Jun 29];28(16). Available from: https://pubmed.ncbi.nlm.nih.gov/22743226/
14. García-Alcalde F, Okonechnikov K, Carbonell J, Cruz LM, Götz S, Tarazona S, et al. Qualimap: evaluating next-generation sequencing alignment data. Bioinform Oxf Engl. 2012;28. Available from: https://pubmed.ncbi.nlm.nih.gov/22914218/
15. Sayols S, Scherzinger D, Klein H. dupRadar: a Bioconductor package for the assessment of PCR artifacts in RNA-Seq data. BMC Bioinform. 2016;17:428.
16. Love MI, Huber W, Anders S. Moderated estimation of fold change and dispersion for RNA-seq data with DESeq2. Genome Biol. 2014;15:550.
17. Lovci M. nugentechnologies/NuMetRRBS. Tecan Genomics. 2021 [cited 2021 Jul 5]. Available from: https://github.com/nugentechnologies/NuMetRRBS
18. Bond CE, Liu C, Kawamata F, McKeone DM, Fernando W, Jamieson S, et al. Oncogenic BRAF mutation induces DNA methylation changes in a murine model for human serrated colorectal neoplasia. Epigenetics. 2018;13:40–8.
19. Leggett B, Whitehall V. Role of the serrated pathway in colorectal cancer pathogenesis. Gastroenterology. 2010;138:2088–100.
20. Fennell L, Dumenil T, Wockner L, Hartel G, Nones K, Bond C, et al. Integrative genome-scale DNA methylation analysis of a large and unselected cohort reveals 5 distinct subtypes of colorectal adenocarcinomas. Cell Mol Gastroenterol Hepatol. 2019;8:269–90.
21. Liu C, Fennell LJ, Bettington ML, Walker NI, Dwine J, Leggett BA, et al. DNA methylation changes that precede onset of dysplasia in advanced sessile serrated adenomas. Clin Epigenetics. 2019;11:90.
22. Bettington M, Rosty C, Whitehall V, Leggett B, McKeone D, Pearson SA, et al. A morphological and molecular study of proposed early forms of traditional serrated adenoma. Histopathology. 2018;73:1023–9.
23. Bettington ML, Walker NI, Rosty C, Brown IS, Clouston AD, McKeone DM, et al. A clinicopathological and molecular analysis of 200 traditional serrated adenomas. Mod Pathol. 2015;28:414–27.
24. McCarthy AJ, Serra S, Chetty R. Traditional serrated adenoma: an overview of pathology and emphasis on molecular pathogenesis. BMJ Open Gastroenterol. 2019;6:e000317.
25. Fennell L, Kane A, Liu C, McKeone D, Hartel G, Su C, et al. *Braf* mutation induces rapid neoplastic transformation in the aged and aberrantly methylated intestinal epithelium. Gut. 2022;71:1127–40.
26. Fennell LJ, Kane A, Liu C, McKeone D, Fernando W, Su C, et al. APC mutation marks an aggressive subtype of BRAF mutant colorectal cancers. Cancers. 2020;12:1171.
27. Bettington M, Walker N, Rosty C, Brown I, Clouston A, McKeone D, et al. Clinicopathological and molecular features of sessile serrated adenomas with dysplasia or carcinoma. Gut. 2017;66:97–106.
28. Nalapareddy K, Nattamai KJ, Kumar RS, Karns R, Wikenheiser-Brokamp KA, Sampson LL, et al. Canonical Wnt signalling ameliorates aging of intestinal stem cells. Cell Rep. 2017;18:2608–21.
29. Cui H, Tang D, Garside GB, Zeng T, Wang Y, Tao Z, et al. Wnt signalling mediates the aging-induced differentiation impairment of intestinal stem cells. Stem Cell Rev Rep. 2019;15:448–55.
30. Pentinmikko N, Iqbal S, Mana M, Andersson S, Cognetta AB, Suciu RM, et al. Notum produced by Paneth cells attenuates regeneration of aged intestinal epithelium. Nature. 2019;571:398–402.
31. Nefzger CM, Jardé T, Srivastava A, Schroeder J, Rossello FJ, Horvay K, et al. Intestinal stem cell aging signature reveals a reprogramming strategy to enhance regenerative potential. npj Regen Med. 2022;7:31.
32. Flanagan DJ, Pentinmikko N, Luopajärvi K, Willis NJ, Gilroy K, Raven AP, et al. NOTUM from Apc-mutant cells biases clonal competition to initiate cancer. Nature. 2021;594:430–5.
33. Mills C. M1 and M2 macrophages: oracles of health and disease. Crit Rev Immunol. 2012;32:463–88.
34. Liu J, Geng X, Hou J, Wu G. New insights into M1/M2 macrophages: key modulators in cancer progression. Cancer Cell Int. 2021;21:389.
35. Najafi M, Hashemi Goradel N, Farhood B, Salehi E, Nashtaei MS, Khanlarkhani N, et al. Macrophage polarity in cancer: a review. J Cell Biochem. 2019;120:2756–65.
36. Conway EM, Pikor LA, Kung SHY, Hamilton MJ, Lam S, Lam WL, et al. Macrophages, inflammation, and lung cancer. Am J Respir Crit Care Med. 2016;193:116–30.
37. Boutilier AJ, Elsawa SF. Macrophage polarization states in the tumor microenvironment. Int J Mol Sci. 2021;22:6995.

AUTHOR CONTRIBUTIONS

LF conceptualised the study, performed animal experiments, analysed bioinformatic data, prepared the manuscript; CL performed histopathological analyses; AK performed animal experiments; ST performed immunohistochemical experiments; JB analysed immunohistochemical data; LC performed bioinformatic analysis; SRD analysed immunohistochemical data; DM performed animal experiments; CB performed animal experiments; BL conceptualised the study, supervised the study; VW conceptualised the study, performed analysis and supervised the study. All authors contributed to review and editing of the manuscript.

FUNDING

Open Access funding enabled and organized by CAUL and its Member Institutions.

COMPETING INTERESTS

The authors declare no competing interests.

ETHICAL APPROVAL

All studies were approved by the QIMR Berghofer Animal Ethics Committee (P2178). All animal experiments were conducted in accordance with institutional and national guidelines and regulations.

ADDITIONAL INFORMATION

Supplementary information The online version contains supplementary material available at https://doi.org/10.1038/s41416-025-03271-3.

Correspondence and requests for materials should be addressed to Lochlan Fennell.

Reprints and permission information is available at http://www.nature.com/reprints

Publisher's note Springer Nature remains neutral with regard to jurisdictional claims in published maps and institutional affiliations.